



Synthesis of NiO/SnO₂ Nanocomposite for Applied as Light Sensitive Electrodes

Zahraa Talib Kadhim⁽¹⁾,

Department of Physics, College of Science, Wasit University, Kut, Iraq

Corresponding authors: zahraatalib2023@gmail.com

Thjeel Al-ogaili ,

Department of Physics, College of Science, Wasit University, Kut, Iraq

Hanan Abd Ali⁽²⁾

Department of Physics, College of Science, Wasit University, Kut, Iraq

ABSTRACT

In this study, nanoparticles for nickel-tin oxide films were prepared using the sol-gel chemical method. Nanocomposite structural and optical properties were studied. X-ray diffraction measurements showed (SnO₂: NiO) (SnO₂ NPs). And the structure was validated to crystallize SnO NPs into hexagonal structure with an average crystal size of 13.80 nm. FE-SEM image study showed the surface morphology of SnO₂: NiO deposition of SnO₂ on a glass substrate. The grain size values for SnO₂ and NiO.SnO₂ NPs range (24 nm and 38.8 μm), respectively. Energy dispersive X-ray spectroscopy (EDS) was analyzed. The amount of nickel tin with oxygen for a sample prepared at room temperature is less than for other samples prepared. These results are consistent with X-ray diffraction analysis, and FE-SEM FT-IR spectroscopy of the as-synthesized NiO NPs, in the wavelength range from 500 to 4500 cm, showed the FT-IR spectrum of the as-synthesized NiO. A broad absorption band is observed at 684.78 cm⁻¹ which is attributed to the Ni-O stretching vibration. The broad peak at 3848.58 cm corresponds to OH. The peaks at 3419.27 and 1637.19 cm were symmetric and asymmetric O-C-O stretching vibrations of the adsorbed carbonate anion, respectively. The peaks at 680.97 and 1637.57 cm⁻¹ are attributed to Sn-O-H expansion caused by impurities of SnO NPs. peak wavelength range (225-550) nm and an increase in the absorption band towards the red wavelength was observed after the addition of nickel oxide. This phenomenon is called the mean value shift. UV-IR analysis showed the band gap energy value (NiO NPs 3.7eV) (SnO₂ NPs 3.3eV) and the band gap value (SnO₂: NiO 3.5eV)

Keywords:

Nanocomposite NiO:SnO₂ , SnO₂ NPs , XRD, SEM,EDX,FTIR ,UV

Introduction

Because of the enhanced surface area to volume ratio, changed structure, and higher activity of nanoparticles over macromolecules, nanoparticle production has received a lot of attention [1 2].

Nanoparticles have a wide range of applications in the optical, electronic, and textile industries, as well as in medicine, cosmetics, and drug delivers [3 223 [3 4]

Nanocomposites are defined as solid materials consisting of at least two phases from which one has a dimension in the nanometer length scale, meaning <100 nm [5]. Nanocomposites are divided into organic or inorganic nanocomposites. Organic compounds may be the resulting amorphous, crystalline, or semi-crystalline materials. Sometimes these nanocomposites exhibit new and improved mechanical, catalytic, electronic, magnetic, and optical properties that are not seen in individual

phases or through their synthesized and micro composite analogues.[6]. Depending upon the dimensions of the dispersed particles, nanocomposites can be categorized into three types. When all the dimensions of the dispersed particles are in the order of nanometers, for example spherical nano-sized particles of silica, various metals, metal oxides, etc., they are referred to as iso-dimensional nanocomposites. In the second category, filler particles with two dimensions in the nanometer scale are employed, e.g. nano tubes, whiskers, etc.

The third type of nanocomposite use particles with only one dimension in the nanometer range, e.g. various layered silicates [7]. The transparent conductive oxides used in this study are

SnO which is an n-type semiconductor with an optical bandgap of 3.4 eV for tin dioxide (SnO₂) has many unique physical properties, such as very high electrical conductivity, as well as high permeability in the ultraviolet visible region, and extraordinary ferromagnetism, so it is considered as a kind of semiconductor, band gap behavior is wide and it is one of the most important transparent conductive oxides. Imported (TCO), (SnO₂) and its alloys have been widely used in photovoltaic devices, solar cells and transparent gas sensors [8] There are several different techniques used to deposition tin dioxide films including chemical vapor deposition [9, 10], pyrolysis by spraying [11, 12], thermal evaporation [13] and spraying [14] The second type of oxides used in our research study is nickel oxide (NiO).

Nickel oxide is usually in the form of a green crystalline powder with a density (6.7 g/cm³) and a melting point (1955 °C) [15]. (NiO) films have a cubic face-shaped crystalline structure similar to that of crystalline sodium chloride (NaCl), and its oxides (NiO_x) are called black nickel oxide, which is a crystalline solid with a melting point of (600 °C) and is used in the manufacture of nickel salts. Substances after tungsten oxide, they are used in the manufacture of electrical anodes because of their high electron density, high stability and durability, malleability, and positive-type (p-type) conductivity [16].

EXPERIMENTAL PROCEDURE MATERIALS

Ni (NO₃)₂·6H₂O, Sn (NO₃)₂·6H₂O, Sodium Hydroxide, (NaOH) and PEG

Preparation of (SnO₂) Nanoparticles

Tin nitrate was taken and dissolved in 50 each of deionized distilled water, Sn (NO₃)₂·6H₂O. The mixture was mixed for 10 minutes at 80 degrees Celsius. NaOH (sodium hydroxide) was added, pH = 9. It precipitated at a temperature of 65 degrees Celsius, while continuing to mix.

The precipitate was filtered and washed several times and dried at 150°C for 2 hours. It was calcined at 600°C for 4 hours. Tin oxide nano powder

Preparation of:(NiO, SnO₂) Nanocomposites

The liquids of SnO₂ and NiO were mixed in proportions by weight of 2 ml of nickel oxide, NiO, and (0.5121 g) of tin oxide, SnO₂. We mixed well on a magnetic stirrer at room temperature for a period of (24-48) hours to stabilize the gel and allow the nanoparticles to grow, after which the NiO gel was separated: SnO₂ from the remaining liquid by filtration. After that, the gel was washed several times with ethanol to remove any unreacted materials or other impurities. The washed gel was dried at a temperature of 80 °C for 4 hours, after that the material was calcined in the oven at a temperature of 600 °C for a period of (2-4) hours to remove any remaining organic matter and improve the crystallization of the NiO:SnO₂ Nanocomposite

Result And Discussions

X-ray diffraction

In X-ray diffraction and crystallography. The Debye-Scherrer equation is a formula that relates crystalline volume in a solid to peak broadening in a diffraction mode. Determine the particle size of the crystals. Therefore, Scherrer's mathematical relation is written in the following form

$$D = (K \lambda) / (\beta \cos \theta) \quad (1)$$

D represents the crystal I size (nm), K is the dimensionless form factor (0.94 for spherical shapes), varies with the actual shape of the crystal, A represents the X-ray wavelength (0.15406 nm), θ is the Bragg diffraction angle (radians), and B. The full width is at the mid-maximum (FWHM) of the selected peak

(radians) The condition that diffraction (peak) occurs for a given set of lattice planes can be easily expressed by drki using the Bragg equation

$$2d_{hkl} \sin\theta = n\lambda \quad (2)$$

The variable (d_{hkl}) represents the distance between the atomic layers in the crystal, (n) is the order and sequence of the diffraction peaks in this equation, and lambda (λ) is the wavelength of the incident X-ray beam.

The peaks in the X-ray diffraction pattern are directly related to the atomic distances in simple structures using the above equations. (2). [17].

The crystal structure of the NiO , SnO₂ and NiO: SnO₂ Nanocomposite was validated using the

XRD technique. The distance between the crystalline levels was determined **Error! Reference source not found.** gives the structural properties of the SnO₂ NPs. **Error! Reference source not found.** show the X-ray diffraction patterns (XRD) of SnO₂. The SnO₂ NPs, diffraction peaks pattern through 2-theta can be well-matched with the miller indices (hkl) at (110), (101) and (211), respectively. This result matches the Crystallography Open Database (COD) card number (96-101-0094). Here, SnO₂ NPs crystallizes in a hexagonal structure with an average crystallite size of 13.80 nm.

Table 1-1 Structural properties of SnO₂ NPs

2θ (Deg.)	FWHM (Deg.)	d.hkl Std.(Å)	dhkl Exp.(Å)	Crystallite size (nm)	Average Crystallite size (nm)
25.27	0.43	3.52	3.52	19.13	13.80
37.80	0.60	2.38	2.38	14.05	
48.03	0.48	1.89	1.89	18.01	
53.95	0.64	1.70	1.70	13.85	
55.04	0.57	1.67	1.67	15.62	
62.66	0.77	1.48	1.48	12.12	
69.59	2.26	1.35	1.35	4.29	
75.12	0.75	1.26	1.26	13.30	

Table Error! No text of specified style in document.-1 Structural properties of NiO: SnO₂ Nanocomposite.

2θ (Deg.)	FWHM (Deg.)	dhkl Std.(Å)	dhkl Exp.(Å)	Crystallite size (nm)	Average Crystallite size (nm)
26.641	0.551	3.4	3.34	14.80	16.30nm
33.935	0.606	2.53	2.64	13.69	
38.031	0.525	2.36	2.36	16.00	
42.679	0.198	2.12	2.12	42.99	
51.87	0.63	1.72	1.76	14.02	
54.82	0.67	1.53	1.67	13.44	
61.99	0.70	1.50	1.50	13.24	
64.80	0.80	1.52	1.44	11.77	
66.03	0.79	1.45	1.41	11.99	
71.42	0.72	1.53	1.32	13.57	
78.82	0.74	1.21	1.21	13.84	

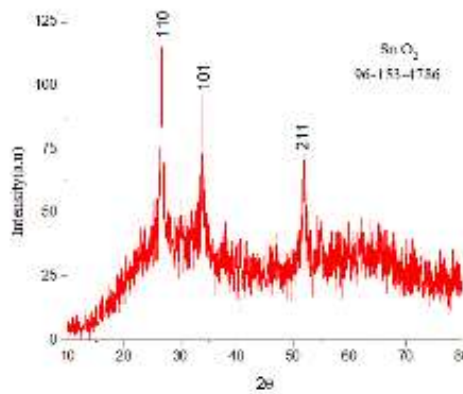
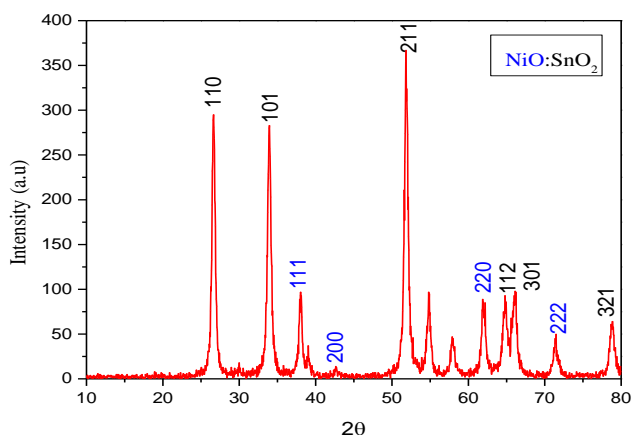


Figure 1.3 XRD pattern of SnO2 NPs

Figure 1.3 XRD pattern of NiO: SnO2

Nanocomposites

Error! Reference source not found. show The NiO: SnO₂ Nanocomposite, diffraction peaks pattern through 2-theta can be well-matched with the miller indices (hkl) at (110), (101), (111), (200), (211),(220),(112),(301),(222) and (321) respectively. This result matches the Crystallography Open Database (COD) card number (96-153-4786 and 96-101-0094). Here, NiO: SnO₂ Nanocomposite with an average crystallite size of 16.30 nm.

Scanning Electron Microscopy (SEM) Analysis

FE-SEM image study shows the surface morphology, SnO₂ and NiO:SnO₂ deposited on

the glass substrate From the morphology picture, it showed that the straight SnO₂ nanostructure is exactly the same except for the presence of a small particle size (24 nm), in addition to the presence of some structures, and crystalline shapes formed by grain agglomerations. And it was found that the NiO:SnO₂ sample has a large grain size (38 μm) compared to the other nanostructured SnO₂ sample as shown from (FE-SEM) images, using (Image J software), the grain size values for SnO₂ and NiO are shown: SnO₂ NPs are in the (24 nm and 38.8 nm) range, respectivel [18]

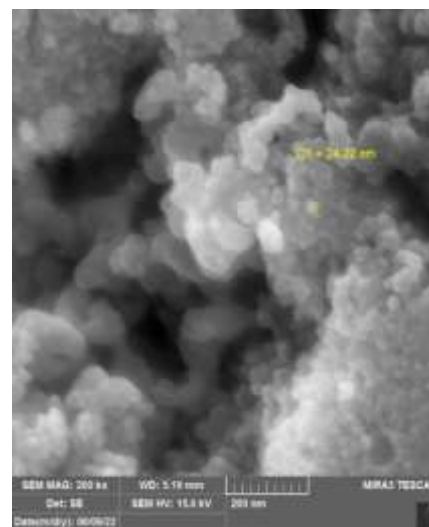
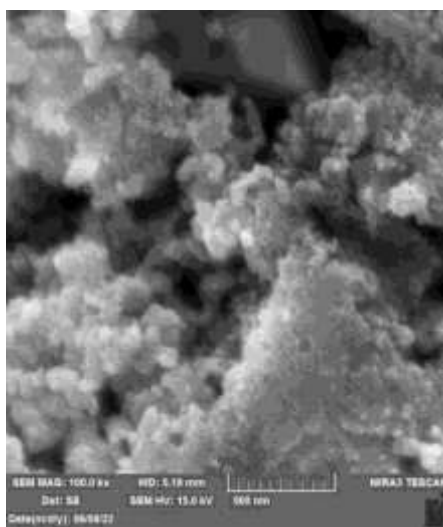
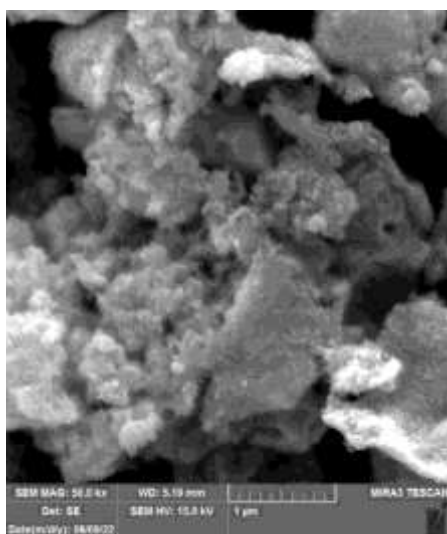


Figure 1-4 SnO₂ Scanning Electron Microscopy (FE-SEM) Analysis show the surface morphology with size about 24nm

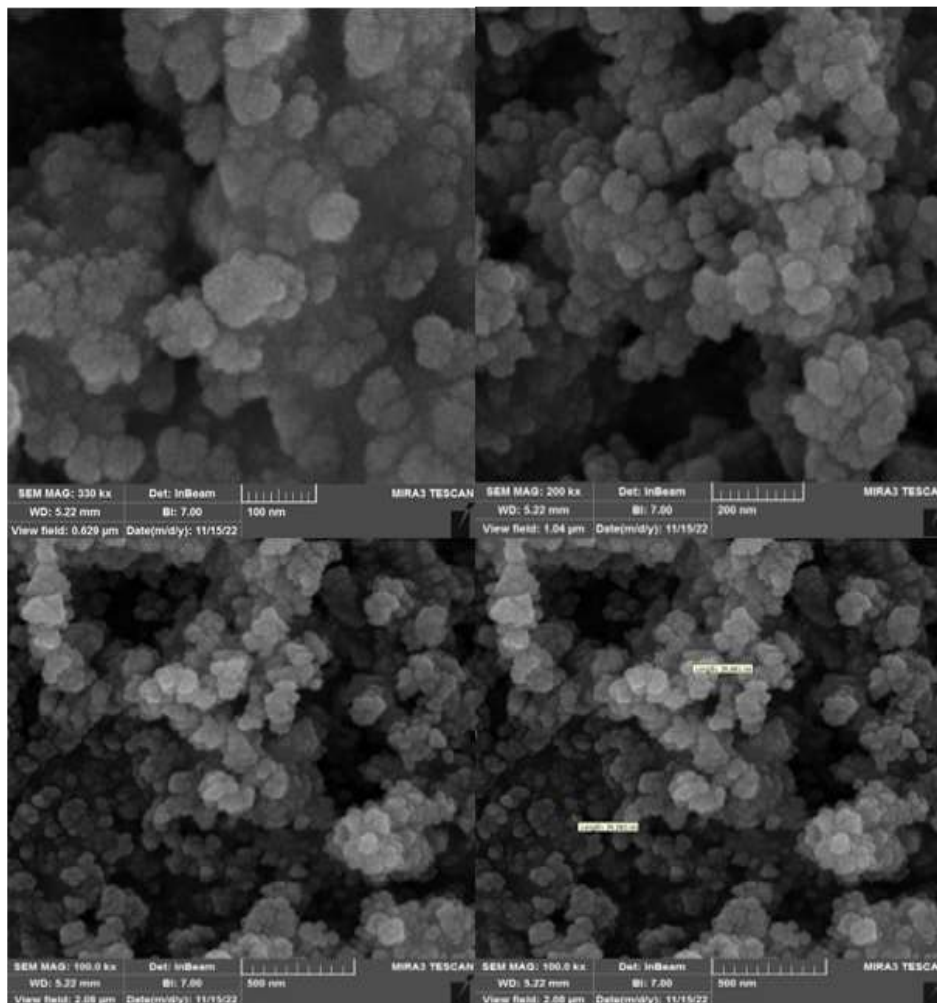


Figure 1.5 NiO: SnO₂ Nanocomposite Scanning Electron Microscopy (FE-SEM) Analysis show the surface morphology

Energy dispersive X-ray spectroscopy (EDS)
 Show energy-dispersive X-ray spectroscopy (EDS), elemental analysis. The results matched the samples that underwent deposition with X-ray diffraction and FE-SEM analysis. He

explained that the characteristics of this thin film in terms of crystal size, grain size, granule size, and porosity are better than other samples prepared under different conditions. and the amount of oxygen in the nanocomposite

Table Error! No text of specified style in document.-2 The ratio of tin Ni, Sn and amount of oxygen in nano composite

			[wt.%]	[at.%]	[wt.%]	
Sn	49	L-series	42.58	57.38	12.59	0.46
O	8	K-series	20.31	27.37	67.65	5.78
Ni	22	K-series	11.31	15.24	19.76	0.46

		Total:	74.2	99.99	100	
--	--	--------	------	-------	-----	--

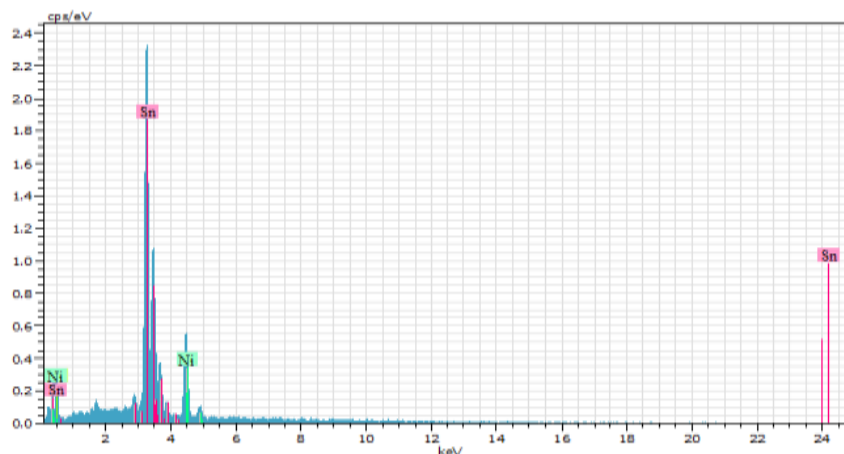


Figure Error! No text of specified style in document..6 EDS analysis of NiO :SnO₂ Figure thin films by chemical technique at room substrates temperature

FT-IR analysis

The Fourier Transform Infrared (FTIR) spectroscopy of SnO₂ its synthesis, such as the formation of precursors, hydrolysis, and condensation reactions. The FTIR spectrum can provide valuable information about the structural changes and bonding that occur during the sol-gel process.

Precursor formation (4000-3200 cm⁻¹): In the initial stages of the sol-gel process, the precursor (typically a metal alkoxide like tin(IV) isopropoxide or tin(IV) ethoxide) is dissolved in a solvent, such as ethanol, and mixed with a water-based solution containing a hydrolyzing agent (e.g., HCl or NH₄OH). The O-H stretching vibrations of the solvent (e.g., ethanol) and water can be observed in the range of 3200-3600 cm⁻¹. The C-H stretching vibrations of the alkoxide group can be detected in the range of 2800-3000 cm⁻¹.

Hydrolysis and condensation (1000-1800 cm⁻¹): During hydrolysis, the alkoxide group (OR) of the precursor reacts with water to form hydroxide (OH) groups. This can be observed as a decrease in the intensity of the C-H and O-C stretching vibrations (1000-1300 cm⁻¹) and the appearance of new peaks corresponding to the Sn-OH stretching vibrations (~800-1000 cm⁻¹).

As condensation proceeds, the intensity of the Sn-OH peaks decreases, and new peaks corresponding to Sn-O-Sn stretching vibrations appear in the range of 400-800 cm⁻¹, indicating the formation of the SnO₂ network. Gelation and drying (400-800 cm⁻¹): As the sol evolves into a gel, the Sn-O-Sn stretching vibrations become more prominent, reflecting the growth of the SnO₂ network. The intensity of the O-H stretching vibrations in the 3200-3600 cm⁻¹ range may also decrease due to the loss of water and solvent during the drying process. Calcination (400-800 cm⁻¹): The final stage in the sol-gel process involves calcination, which involves heating the dried gel at high temperatures (typically 400-800°C) to remove any remaining organic residues and improve the crystallinity of the SnO₂. After calcination, the FTIR spectrum should display a well-defined peak corresponding to the Sn-O-Sn stretching vibrations in the range of 400-800 cm⁻¹, indicating the formation of crystalline SnO₂. The disappearance of the O-H stretching vibrations in the 3200-3600 cm⁻¹ range and the C-H and O-C stretching vibrations in the 1000-1300 cm⁻¹ range confirms the removal of organic residues and completion of the sol-gel process.

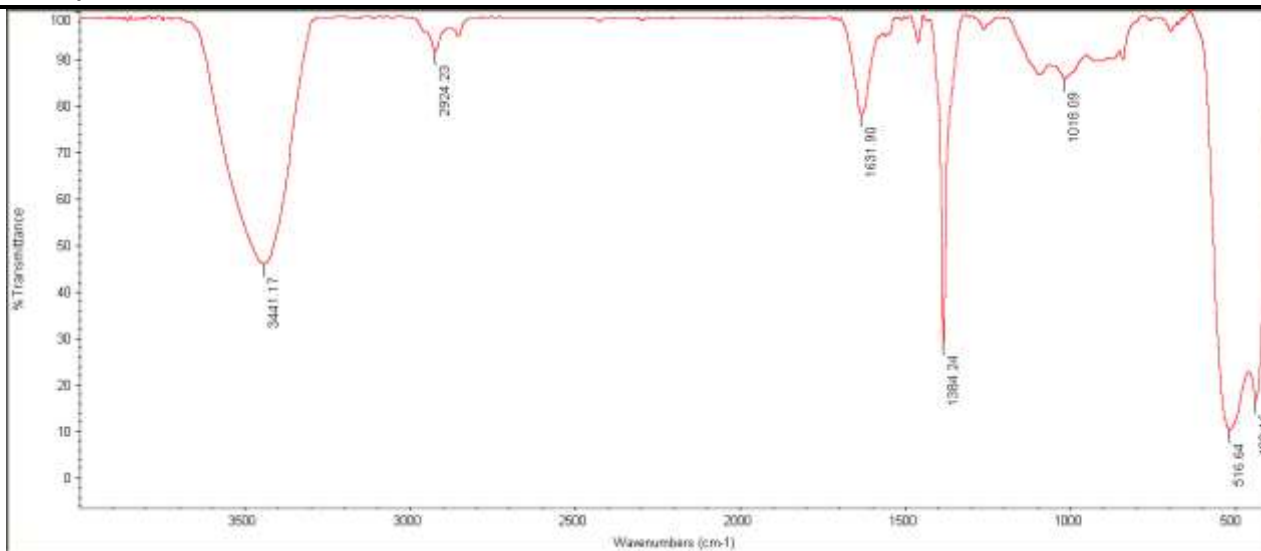


Figure 1.7 FT-IR spectrum of synthesized SnO2 NPs

The spectra showed that the peaks at 3848.77 and 680.97 cm⁻¹ are typical stretching vibrations for hydroxyl groups. The intense peaks at 2078.70 cm⁻¹ indicate the asymmetric and symmetric stretching vibrations C-O due to C-OH groups. Weaker double peaks located at 3848.77 cm⁻¹ give rise to C-O-C symmetrical stretching vibrations. Also, the peaks at 680.97

and 1637.57 cm⁻¹ indicate Sn-O-H expansion caused by Sn(OH) impurities. The most important differences and comparison between the three treatments are the peaks at 3424.60 cm⁻¹ and 2078.70 cm⁻¹ and the peaks less than 1000 cm⁻¹ resulted in Sn-O-Sn expansion. coordination mode between Ni and SnO₂ also shifts against that of pure SnO₂[19]

Table 1-3 peak of NiO: SnO₂ nanocomposite from FTIR spectrum

Peak Number	X (cm-1)	Y (%T)
1	3848.77	93.82
2	3424.60	5.43
3	2078.70	88.41
4	1637.57	38.99
5	680.97	72.41

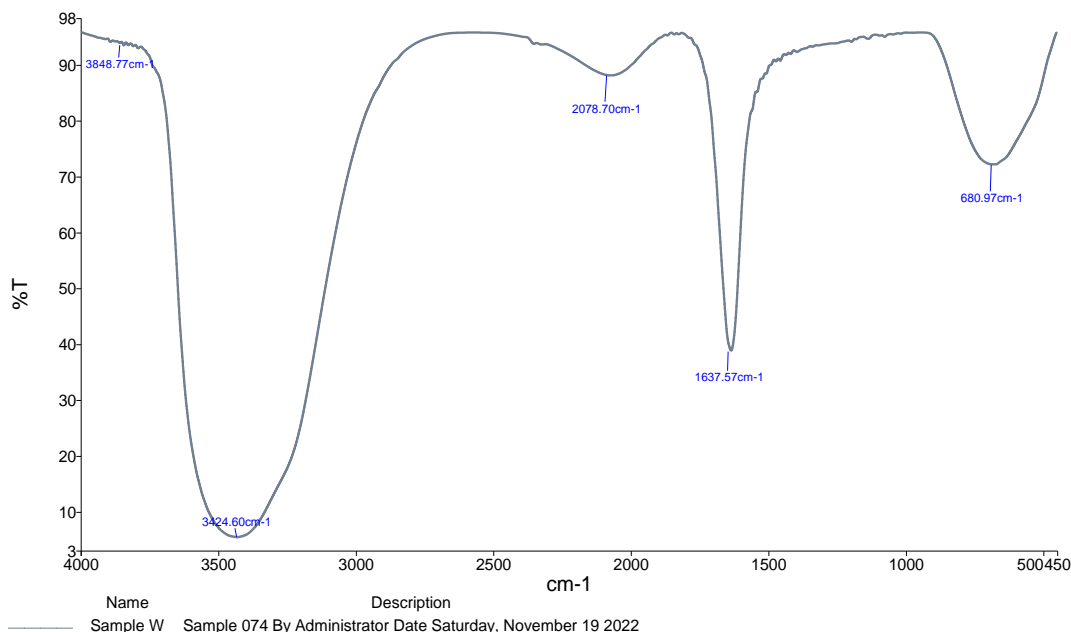


Figure 1.8 FT-IR spectrum of synthesized NiO: SnO₂ nanocomposite

Study of the Optical Properties

Absorbance Spectra Measurement

the UV-Spectral absorption of NiO NPS. It is seen that the maximum peak range of wavelength (200-300) nm and **Error! Reference source not found.** shows the UV-Spectral absorption of NiO: SnO₂ NPS the peak range of wavelength (225-550) nm and notice an increase in the

absorption range towards the red wavelength after adding nickel oxide, and this phenomenon is called red-shifting. This phenomenon can be clearly seen in which shows the improvement in the susceptibility of the resulting material from adding nickel oxide to tin oxide by improving the extent of absorbance in the aforementioned sample

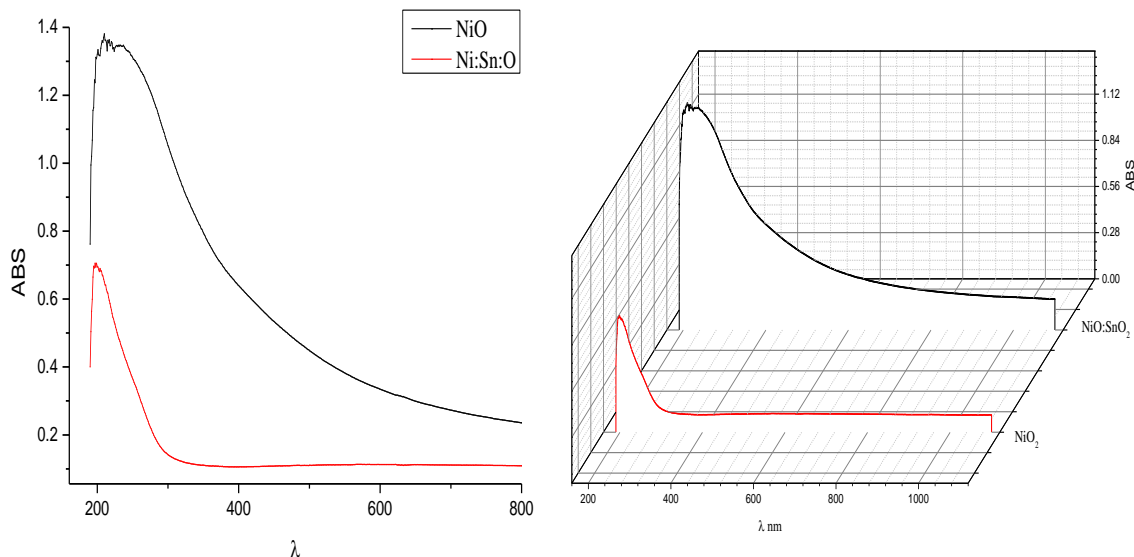


Figure Error! No text of specified style in document..9 shows the UV-Spectral absorption of NiO NPs and NiO: SnO₂ Nanocomposite

The UV-Spectral absorption of NiO NPS. It is seen that the maximum peak range of wavelength (200-300) nm and **Figure Error!** No text of specified style in document..9 shows the UV-Spectral absorption of NiO: SnO₂ NPS the peak range of wavelength (225-550) nm and notice an increase in the absorption range towards the red wavelength after adding nickel oxide, and this phenomenon is called red-shifting. This phenomenon can be clearly seen in which shows the improvement in the susceptibility of the resulting material from adding nickel oxide to tin oxide by improving the extent of absorbance in the aforementioned sample

Energy gap estimation

The optical transmittance of the samples was recorded at room temperature within the wavelength range (200-1100 m). Transmittance measurements of SnO and NiO:SnO thin films were performed using a different substrate. reactant. The plot between $(\alpha h\nu)^2$ and $h\nu$ shows a straight line, and extrapolating the straight line to $(\alpha h\nu)^2 = 0$ results in the amount of the band gap for the sample. The energy gap value for NiO is in the range (3.7ev), as well as the energy gap for tin oxide within the range (3.3ev). ev) and the thin film energy gap of the NiO:SnO₂ nanocomposite is (3.5ev) [20]

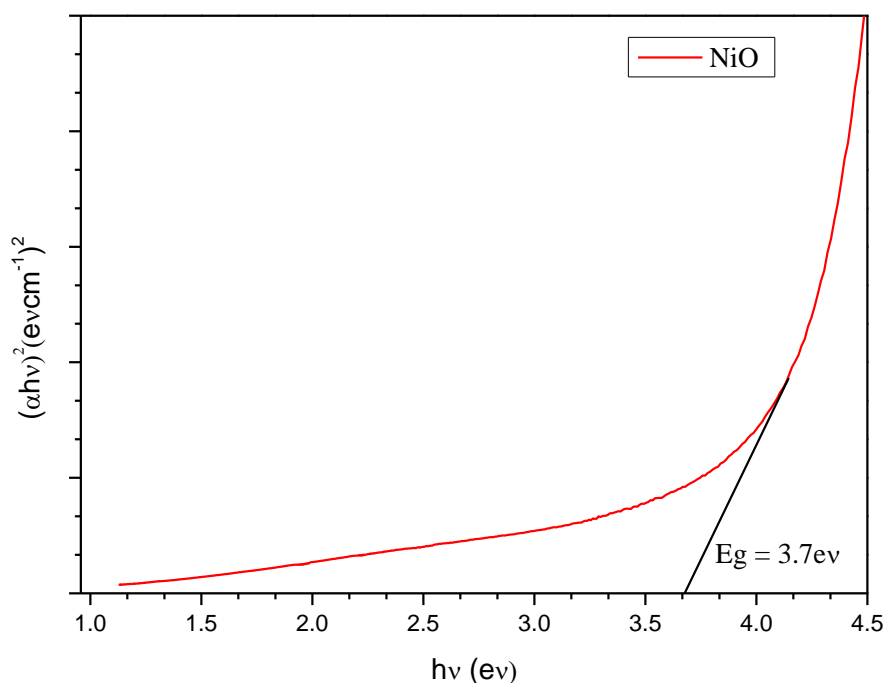


Figure1.10 Energy bandgap (Eg) of the, NiO

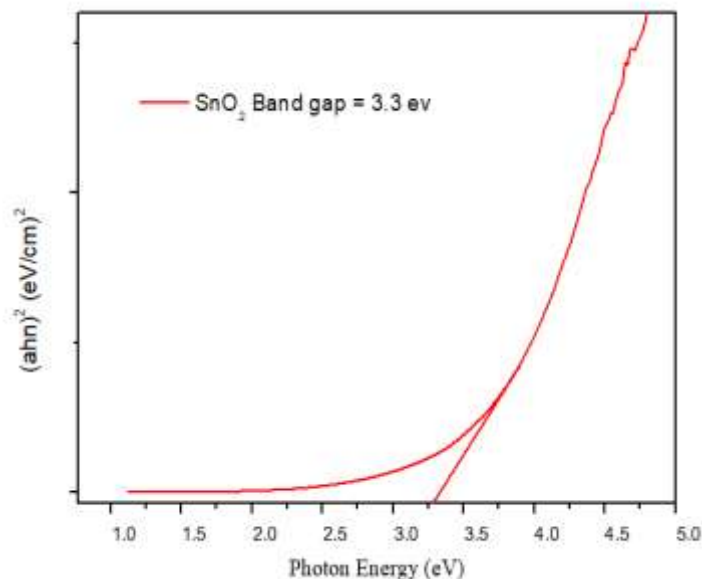


Figure 1.11 Show the band gap of SnO₂ NPs at the range of (3.3 ev

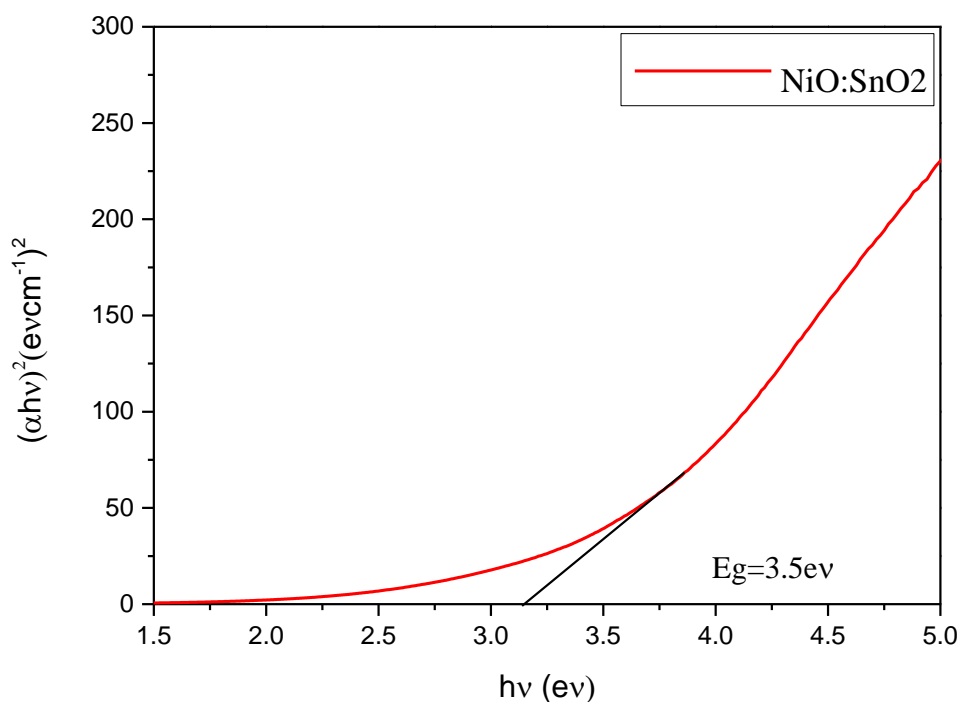


Figure Error! No text of specified style in document..12 .Energy bandgap (Eg) of the, NiO: SnO₂ Nanocomposite

The doping of the samples with nickel oxide led to an increase in the energy gap, which is associated with a decrease in the size of the nanoparticles. This result is very compatible with the results of the diagnosis using electron

microscopy and X-ray diffraction examination, which confirm the consistency of the results.

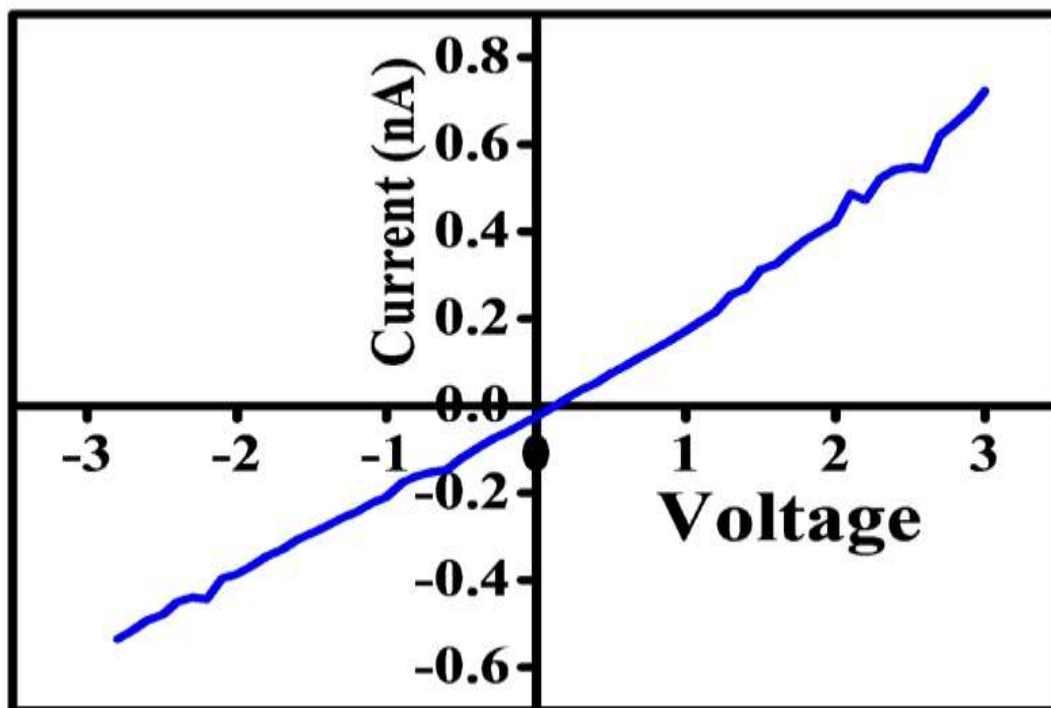
Photosensitive electrodes Application

Figure 1.10 show Current vs. Voltage characteristics of Chemical synthesized: SnO₂

nanoparticles shows the current vs voltage plot of chemical-synthesized NiO:SnO₂ nanoparticles coated onto glass substrates using dip coating method. From the figure it can

be seen that the NiO:SnO₂ nanoparticle thin film shows ohmic nature. The current through the thin film is found to be in nano Ampere.

Figure Error! No text of specified style in document..12 Current vs. Voltage characteristics of Chemical synthesized: SnO₂ nanoparticles.



References: -

1. Dror-Ehre, H. Mamane, T. Belenkova, G. Markovich, and A. Adin, Silver nanoparticle-E. coli colloidal interaction in water and effect on E. coli survival, *J. Colloid Interface Sci.*, 339, 2, 521-526 (2009).
2. S. Prashanth, I. Menaka, R. Muthezhilan, and N. K. Sharma, Synthesis of plant-mediated silver nano particles using medicinal plant extract and evaluation of its anti microbial activities, *Int J Eng Sci Technol*, 3, 6235-6250 (2011).
3. G. R. Bardajee, Z. Hooshyar, and H. Rezanezhad, A novel and green biomaterial based silver nanocomposite hydrogel: Synthesis, characterization and antibacterial effect, *J. Inorg. Biochem.*, 117, 367-373 (2012).
4. M. Bin Ahmad, J. J. Lim, K. Shameli, N. A. Ibrahim, M. Y. Tay, and B. W. Chieng, Antibacterial activity of silver bionanocomposites synthesized by chemical reduction route, *Chem. Cent. J.*, 6, 1, 1-9 (2012)
5. Guglielmi M., Kickelbick G. and Martucci A., "Sol-Gel Nanocomposites",
6. Springer science and business media Singapore, 2014.
7. Thomas S. and Stephen R., "Rubber Nanocomposites: Preparation,
8. Properties, and Applications ", John Wiley & Sons, 2010.
9. Thomas S., Chan C. H., Pothen L. A., J. P Joy and H. J. Maria," Natural
10. Rubber Material", Second Volume, Royal Society of Chemistry, 2013
11. K. Chopra, s. Major, and D. J. T. s. f. Pandya, "Transparent conductors--a status review," vol.102, no. 1, pp. 1-46, 1983.
12. O. S. Heavens, Optical properties of thin solid films. Courier Corporation, 1991.

13. A. Rakhshani, Y. Makdisi, and H. J. J. o. a. p. Ramazaniyan, "Electronic and optical properties of fluorine-doped tin oxide films," vol. 83, no. 2, pp. 1049-1057, 1998.
14. A. I. Martinez and D. R. J. T. s. f. Acosta, "Effect of the fluorine content on the structural and electrical properties of SnO₂ and ZnO–SnO₂ thin films prepared by spray pyrolysis," vol. 483, no. 1-2, pp. 107-113, 2005.
15. B. J. T. s. f. Thangaraju, "Structural and electrical studies on highly conducting spray deposited fluorine and antimony doped SnO₂ thin films from SnCl₂ precursor," vol. 402, no. 1-2, pp. 71-78, 2002.
16. D. Das and R. J. T. s. f. Banerjee, "Properties of electron-beam-evaporated tin oxide films," vol. 147, no. 3, pp. 321-331, 1987.
17. M. Dwech and K. J. j. o. k. u. Aadim, "Structural and Optical Properties of SnO₂: MgO Thin Films Preparing by Pulse Laser Deposition Technique at 423K," vol. 11, no. 1, pp. 293-302, 2015
18. A. Bakry and S. Mahmoud, "Effect of substrate temperature on the optical dispersion of sprayed nickel oxide thin films," in *2011 Saudi International Electronics, Communications and Photonics Conference (SIECPC)*, 2011: IEEE, pp. 1-7.
19. A. Y. S. Abu-Yaqoub, "Electrochromic Properties of Sol-gel NiO–based films," 2012.
20. P. Patil and L. J. A. s. s. Kadam, "Preparation and characterization of spray pyrolyzed nickel oxide (NiO) thin films," vol. 199, no. 1-4, pp. 211-221, 2002
21. Z. Moore, Application of x-ray diffraction methods and molecular mechanics simulations to structure determination and cotton fiber analysis. University of New Orleans, (2008).
22. A. Rahdar, M. Aliahmad, and Y. Azizi, "NiO nanoparticles: synthesis and characterization," 2015.
23. C. Terrier, J. Chatelon, and J. Roger, "Electrical and optical properties of Sb: SnO₂ thin films obtained by the sol-gel method," *Thin solid films*, vol. 295, no. 1-2, pp. 95-100, 1997.
24. [21] Adiba, V. Pandey, S. Munjal, and T. Ahmad, "Structural and optical properties of sol gel synthesized NiO nanoparticles," in *AIP Conference Proceedings*, 2020, vol. 2270, no. 1: AIP